Chemical composition of nanoparticles from α-pinene nucleation and the influence of isoprene and relative humidity at low temperature

Lucía Caudillo[1], Birte Rörup[2], Martin Heinritzi[1], Guillaume Marie[1], Mario Simon[1], Andrea C. Wagner[3], Tatjana Müller[1,4], Manuel Granzin[1], Antonio Amorim[5], Farnoush Ataei[6], Rima Baalbaki[2], Barbara Bertozzi[7], Zoé Brasseur[2], Randall Chiu[3], Biwu Chu[2], Lubna Dada[8], Jonathan Duplissy[2,9], Henning Finkenzeller[3], Loïc Gonzalez Carracedo[10], Xu-Cheng He[2], Victoria Hofbauer[11], Weimeng Kong[12,13], Houssni Lamkaddam[8], Chuan P. Lee[8], Brandon Lopez[11], Naser G. A. Mahfouz[11], Vladimir Makhmutov[14,26], Hanna E. Manninen[15], Ruby Marten[8], Dario Massabò[16], Roy L. Mauldin[17,11], Bernhard Mentler[18], Ugo Molteni[8,20,21], Antti Onnela[15], Joschka Pfeifer[15], Maxim Philippov[14], Ana A. Piedehierro[22], Meredith Schervish[11], Wiebke Scholz[18], Benjamin Schulze[12], Jiali Shen[2], Dominik Stolzenburg[2], Yuri Stozhkov[14], Mihnea Surdu[8], Christian Tauber[10], Yee Jun Tham[2], Ping Tian[23], António Tomé[24], Steffen Vogt[7], Mingyi Wang[11], Dongyu S. Wang[8], Stefan K. Weber[15], André Welti[22], Wang Yonghong[2], Wu Yusheng[2], Marcel Zauner-Wieczorek[1], Urs Baltensperger[8], Imad El Haddad[8], Richard C. Flagan[12], Armin Hansel[18,19], Kristina Höhler[7], Jasper Kirkby[1,15], Markku Kulmala[2,9,25], Katrianne Lehtipalo[2,22], Ottmar Möhler[7], Harald Saathoff[7], Rainer Volkamer[3], Paul M. Winkler[10], Neil M. Donahue[11], Andreas Kürten[1], Joachim Curtius[1].

[1]Institute for Atmospheric and Environmental Sciences, Goethe University Frankfurt, 60438 Frankfurt am Main, Germany
[2]Institute for Atmospheric and Earth System Research (INAR) / Physics, Faculty of Science, University of Helsinki, 00014 Helsinki, Finland
[3]Department of Chemistry & CIRES, University of Colorado Boulder, Boulder, CO, 80309-0215, USA
[4]Max Planck Institute for Chemistry, Mainz, 55128, Germany
[5]CENTRA and FCUL, University of Lisbon, 1749-016 Lisbon, Portugal
[6]Leibniz Institute for Tropospheric Research, Leipzig, 04318, Germany
[7]Institute of Meteorology and Climate Research, Karlsruhe Institute of Technology, 76344 Eggenstein-Leopoldshafen, Germany
[8]Laboratory of Atmospheric Chemistry, Paul Scherrer Institute, 5232 Villigen, Switzerland
[9]Helsinki Institute of Physics, University of Helsinki, 00014 Helsinki, Finland
[10]Faculty of Physics, University of Vienna, 1090 Vienna, Austria
[11]Center for Atmospheric Particle Studies, Carnegie Mellon University, Pittsburgh, PA, 15213, USA
[12]Division of Chemistry and Chemical Engineering, California Institute of Technology, Pasadena, CA 91125, USA
[13]California Air Resources Board, Sacramento, CA, 95814, USA
[14]Lebedev Physical Institute, Russian Academy of Sciences, 119991, Moscow, Russia
[15]CERN, 1211 Geneva, Switzerland
[16]Dipartimento di Fisica, Università di Genova and INFN, 16146 Genova, Italy
[17]Department of Atmospheric and Oceanic Sciences, University of Colorado Boulder, Boulder, CO 80309, USA
[18]Institute for Ion and Applied Physics, University of Innsbruck, 6020 Innsbruck, Austria
[19]Ionicon Analytik GmbH, 6020 Innsbruck, Austria
[20]Forest Dynamics, Swiss Federal Institute for Forest, Snow and Landscape Research, 8903 Birmensdorf, Switzerland
[21]Department of Chemistry, University of California, Irvine, Irvine, CA 92697, USA
[22]Finnish Meteorological Institute, 00560 Helsinki, Finland
[23]Beijing Weather Modification Office, China
[24]IDL, Universidade da Beira Interior, R. Marquês de Ávila e Bolama, Covilhã, 6201-001, Portugal

[25]Aerosol and Haze Laboratory, Beijing Advanced Innovation Center for Soft Matter Science and Engineering, Beijing University of Chemical Technology, Beijing, 100029, P.R. China
[26]Moscow Institute of Physics and Technology (National Research University), 117303, Moscow, Russia

Correspondence to: Lucía Caudillo (lucia.caudillo@iau.uni-frankfurt.de) and Joachim Curtius (curtius@iau.uni-frankfurt.de)

Supplementary Material
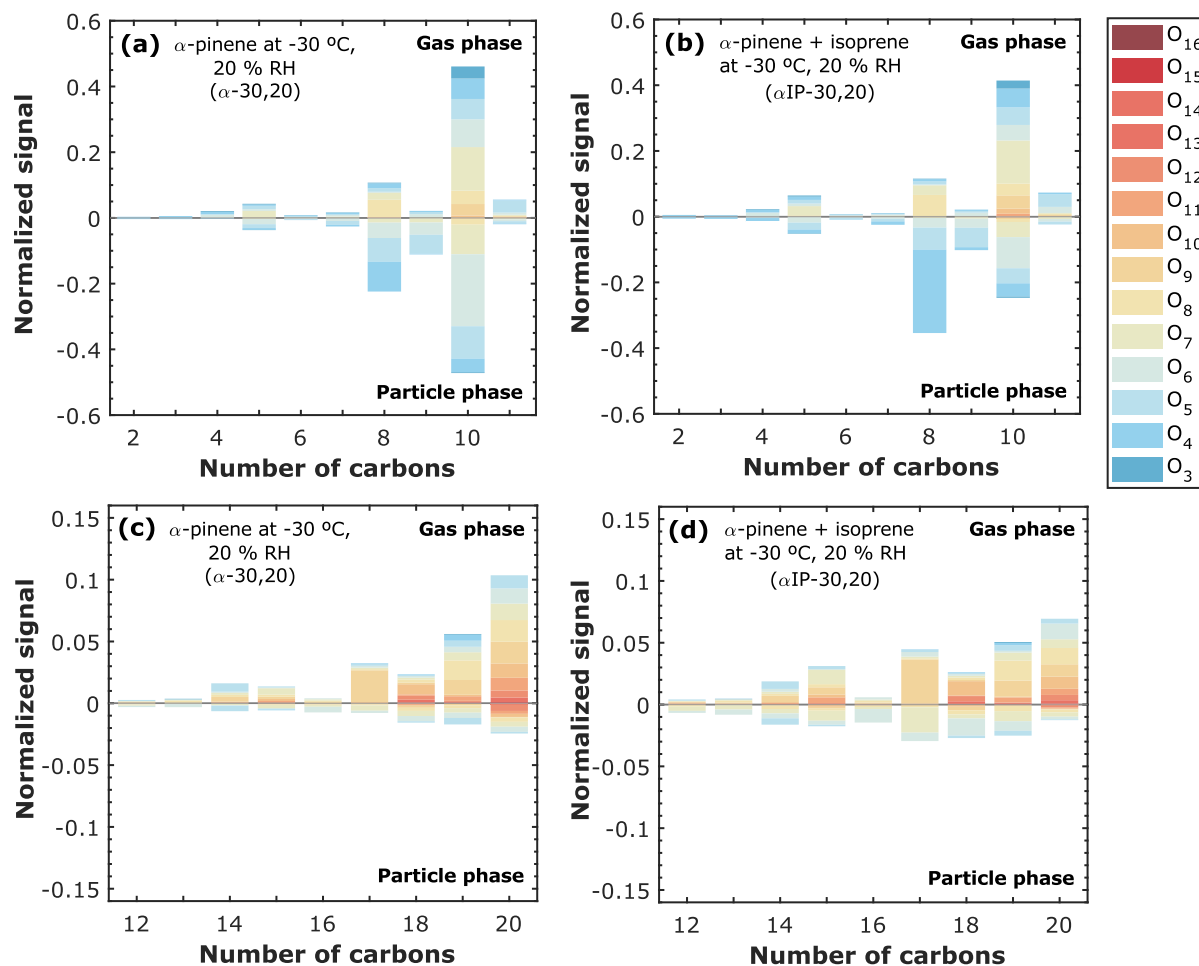
Figure S1. Carbon atom distribution C_{2-11} and C_{12-20} and oxygen atom content in gas and particle phase molecules. Both phases are measured with a Nitrate CI-APi-TOF Mass Spectrometer, while the TD-DMA is coupled to it for particle phase measurements. (a) and (c) α-pinene oxidation products at -30 °C and 20 % RH (α-30,20), (b) and (d) α-pinene + isoprene oxidation products at -30 °C and 20 % RH (αIP-30,20). The level of α-pinene was between 1 and 8 ppbv in (a) (b) (c) and (d), while isoprene level reached up to 30 ppbv in (b) and (d). Ozone level was stable at ~ 100 ppbv for all the experiments. The intensities are normalized by the total signal in each system. Each color represents a specific number of oxygen atoms in the range of 3 to 16.
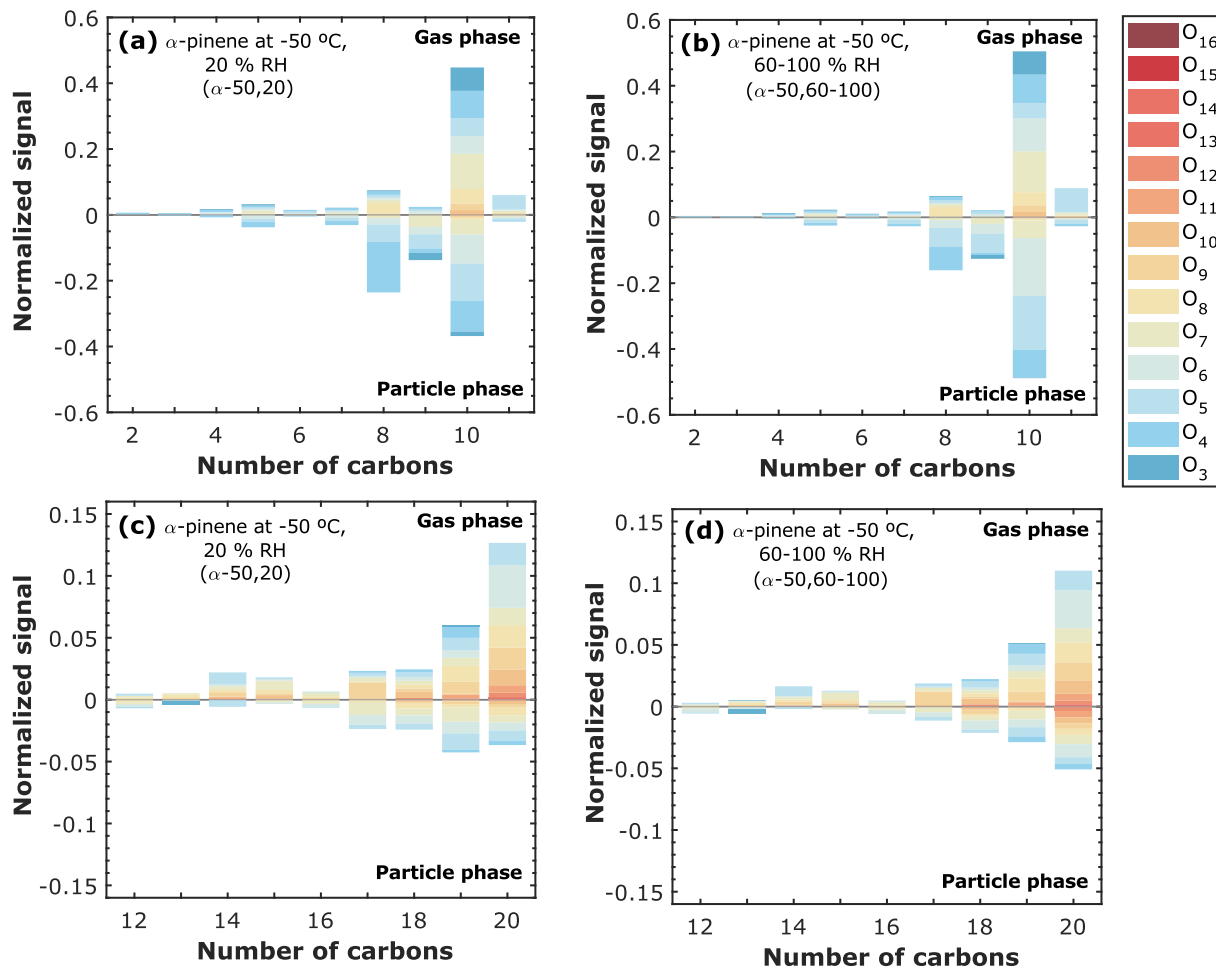
Figure S2. Carbon atom distribution C_{2-11} and C_{12-20} and oxygen atom content in gas and particle phase molecules. Both phases are measured with a Nitrate CI-APi-TOF Mass Spectrometer, while the TD-DMA is coupled to it for particle phase measurements. (a) and (c) α-pinene oxidation products at -50 °C and 20 % RH (α-50,20), (b) and (d) α-pinene oxidation products at -50 °C and 60-100 % RH (α-50,60-100). The level of α-pinene was between 1 and 8 ppbv and Ozone level was stable at ~ 100 ppbv for all the experiments. The intensities are normalized by the total signal in each system. Each color represents a specific number of oxygen atoms in the range of 3 to 16.
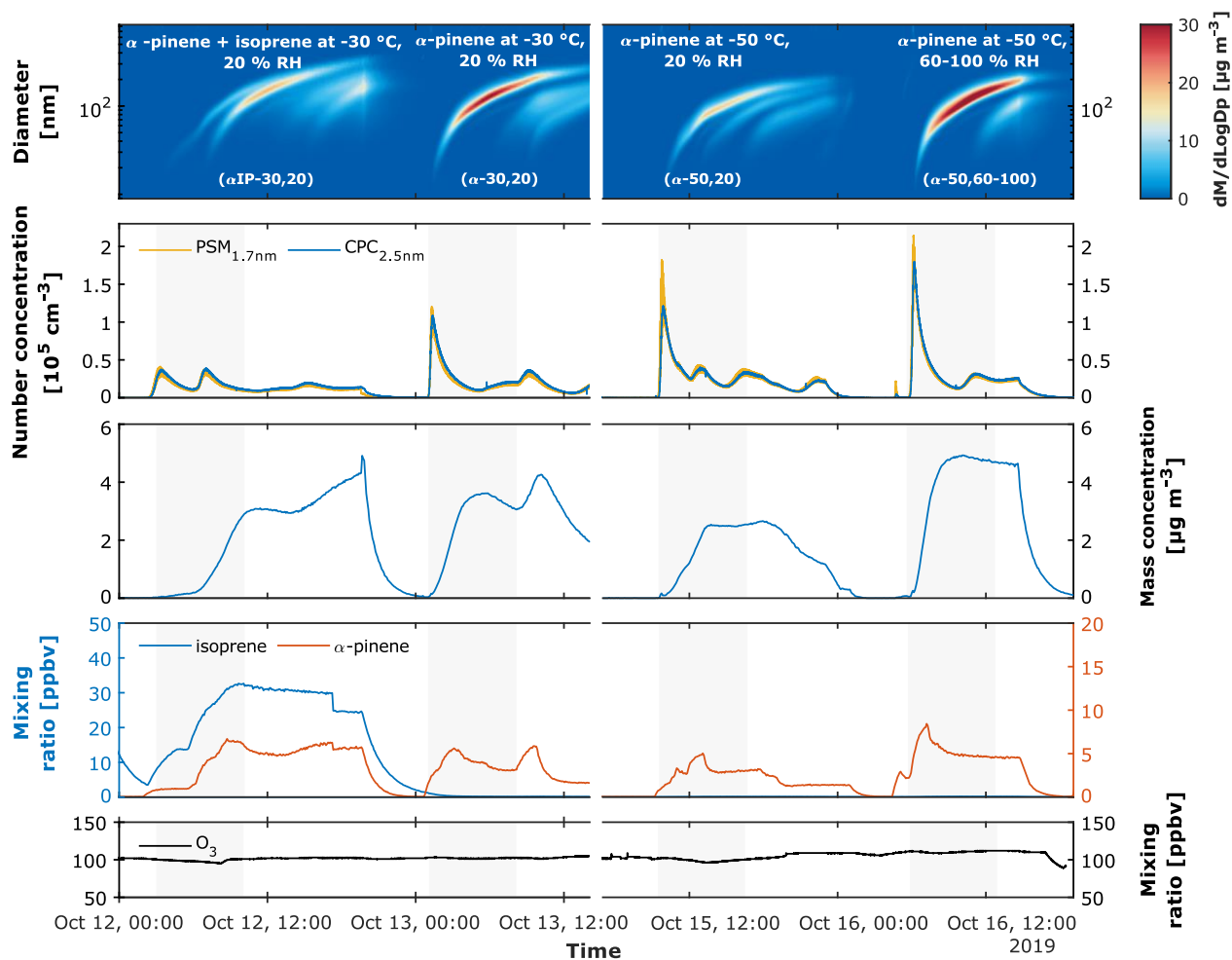
Figure S3. Experimental overview for pure biogenic new particle formation. First panel: particle size distribution for four different experiments: α-pinene + isoprene at -30 °C and 20 % RH (αIP-30,20); α-pinene at -30 °C and 20 % RH (α-30,20); α-pinene at -50 °C and 20 % RH (α-50,20) and α-pinene at -50 °C and 60-100 % RH (α-50,60-100). The color scale represents the normalized mass concentration in μg m⁻³. Second panel: Particle number concentration in cm⁻³ measured by the PSM with a cut-off diameter of 1.7 nm and CPC with a cut-off diameter of 2.5 nm. Third panel: Mass concentration in μg m⁻³ (obtained by integrating the normalized mass concentration from the SMPS). Fourth panel: Mixing ratio in ppbv for the biogenic precursor gases, isoprene and α-pinene. Fifth panel: Ozone mixing ratio in ppbv. The shaded areas refer to the time where the particles were collected using the TD-DMA.
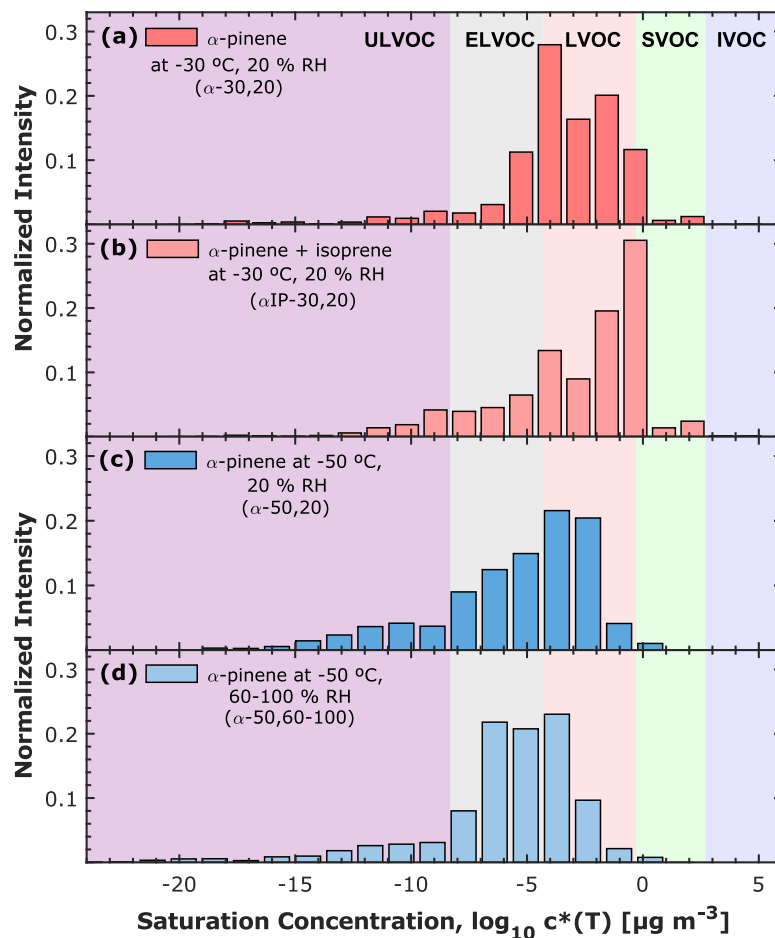
Figure S4. TD-DMA Volatility distribution of the measured oxidation products in the particle phase for four different experiments: (a) α-pinene at -30 °C and 20 % RH (α-30,20); (b) α-pinene + isoprene at -30 °C and 20 % RH (αIP-30,20); (c) α-pinene at -50 °C and 20 % RH (α-50,20) and (d) α-pinene at -50 °C and 60-100 % RH (α-50,60-100). Every individual volatility bin includes the sum of the intensity for the oxidation products normalized by the total signal in each system. Every individual volatility bin is defined at 300 K, shifted, and widened according to their corresponding temperature. The color bands in the background indicate the volatility regimes as in Donahue et al. (2012) and in Schervish and Donahue (2020). The normalized intensity is dimensionless. Nevertheless, it should be noted that the particle phase signal is given in normalized counts per second integrated over the evaporation time [ncps. s].
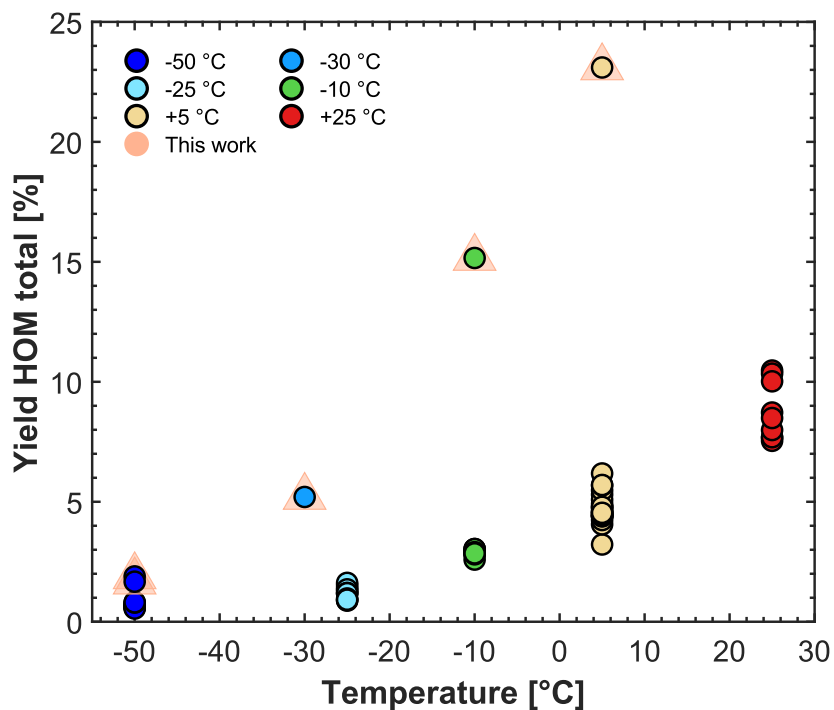
Figure S5. Yield of total HOM as a function of temperature for pure α-pinene systems. Data points at -50 °C, -25 °C, -10 °C, +5 °C and +25 °C are from Simon et al. (2020) and the data points with the orange shadows are the contribution of this study (α-30,20, α-50,20 and α-50,60-100 and complementary pure α-pinene experiments at +5 °C and at -10 °C). The level of precursor gases from Simon et al., (2020) were 0.2 to 0.8 ppbv for α-pinene and 40 to 50 ppbv for ozone, while for experiments reported here (shown with orange shadows), the mixing ratios were 1 to 8 ppbv for α-pinene and 100 ppbv for ozone.
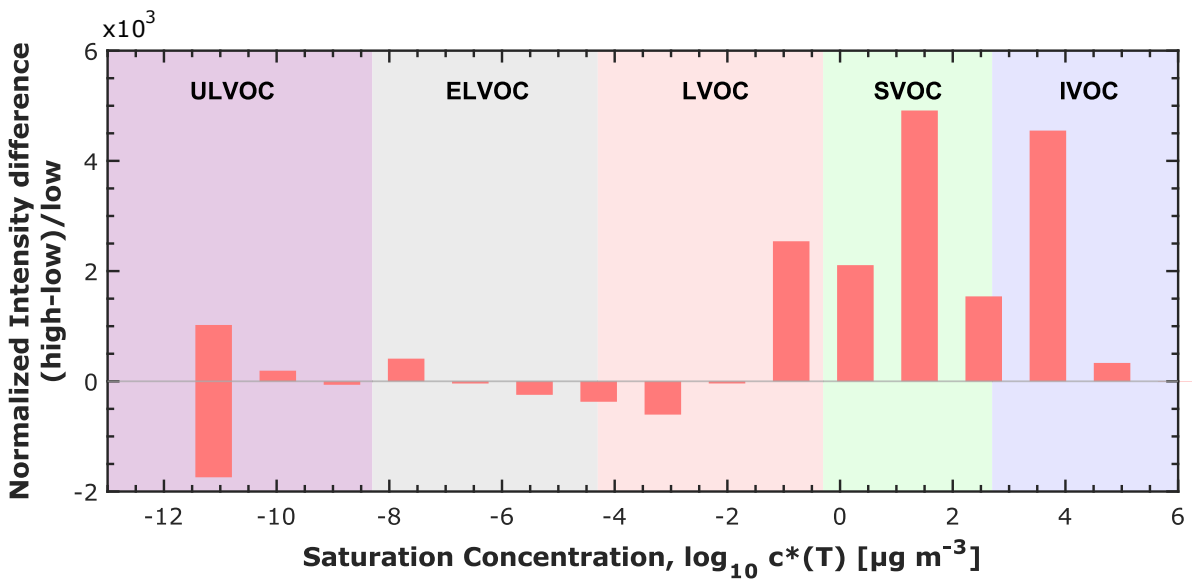
90

Figure S6. Volatility distribution of gas phase for two different systems and the normalized difference between them. Gas phase is measured with a Nitrate CI-APi-TOF Mass Spectrometer. Every individual volatility bin includes the normalized intensity difference (high-low)/low, which is calculated based on intensity of the system at high level of precursor gases (α-pinene was 2 - 3 ppbv and Ozone ~ 100 ppbv) and on the system at low level of precursor gases (α-pinene was 0.2 - 0.8 ppbv and Ozone ~ 40 - 50

95   **ppbv). Every individual volatility bin is defined at 300 K, shifted, and widened according to their corresponding temperature. The lowest bin is an overflow bin. The color bands in the background indicate the volatility regimes as in Donahue et al. (2012) and in Schervish and Donahue (2020).**
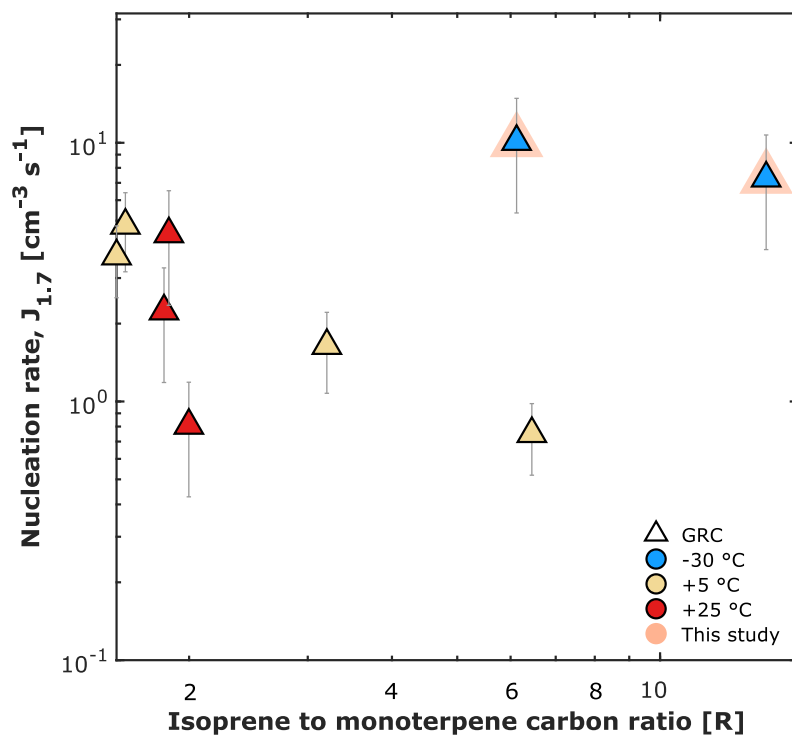
 Figure S7. Pure biogenic nucleation rates at 1.7 nm diameter against isoprene-to-monoterpene carbon ratio (R) at different temperatures. Triangles represent Galactic Comic Rays (GCR) conditions. Data points at +5 °C and +25 °C are from Heinritzi et al., (2020). The points with the orange shadows are the experiments reported in this study for α-pinene + isoprene oxidation products at -30 °C and 20 % RH (αIP-30,20).